ISSN 1028-334X, Doklady Earth Sciences, 2006, Vol. 411A, No. 9, pp. 1341–1345. © Pleiades Publishing, Inc., 2006.
Original Russian Text © Yu.L. Ronkin, D.V. Grazhdankin, A.V. Maslov, G.A. Mizens, D.I. Matukov, M.T. Krupenin, G.A. Petrov, O.P. Lepikhina, A.Yu. Kornilova, 2006, published in Doklady Akademii Nauk, 2006, Vol. 411, No. 3, pp. 354–359.

GEOLOGY

U–Pb (SHRIMP II) Age of Zircons from Ash Beds of the Chernokamen Formation, Vendian Sylvitsa Group (Central Urals)

Yu. L. Ronkin[a], D. V. Grazhdankin[b], Corresponding Member of the RAS A. V. Maslov[a], G. A. Mizens[a], D. I. Matukov[c], M. T. Krupenin[a], G. A. Petrov[a], O. P. Lepikhina[a], and A. Yu. Kornilova[a]

Received April 7, 2006

DOI: 10.1134/S1028334X06090029

The Serebryanka and Sylvitsa groups on the western slope of the Urals characterize the Vendian section of the eastern folded framework of the East European Platform [1]. They are conspicuous against the background of the coeval platformal sequences by their relatively complete sedimentary record, sufficiently good outcrops, and opportunities for detailed sedimentological study both along and across the regional paleoslope. The tillite units serve as key elements of the stratigraphic framework of the Serebryanka Group. However, their number and continuity along the strike remain a matter of debate [1, 2]. The Sylvitsa Group comprises the following formations recognized on a regional scale (from bottom to top): Staropechny Formation (with a thin tillite unit at the base), Perevalok, Chernokamen, and Ust'-Sylvitsa formations. Their specific structural features serve as criteria for large-scale correlation with Upper Vendian platformal sequences [1–3].

The Ediacaran-type soft-bodied fossil biota is abundant in the Chernokamen Formation. The great density of fossil populations, the high taxonomic diversity of this biota, and the presence of endemic (for the Southeast White Sea region) taxons give grounds to suggest biogeographic links between the Central Ural and White Sea segments of the Late Vendian paleobasin [4]. The fossil biota from sedimentary rocks of the Chernokamen Formation comprises *Cyclomedusa davidi* Sprigg, *Dickinsonia* sp., *Dickinsonia tenuis* Glaessner et Wade, *Ediacaria flindersi* Sprigg, *Eoporpita medusa* Wade, *Inaria khatyspytia* (Vodanjuk), *Irridinitus multiradiatus* Fedonkin, *Medusinites mawsoni* (Sprigg), *Nemiana simplex* Palij, *Paliella patelliformis* Fedonkin, *Palaeopascichnus delicatus* Palij, *Protodipleurosoma wardi* Sprigg, *Vaizitsinia sophia* Sokolov et Fedonkin, and *Yorgia* sp. These data make it possible to correlate the Chernokamen Formation of the Central Urals with the reference section of the southeastern White Sea region. The Upper Vendian of the White Sea region includes a very characteristic taxon *Yorgia*, which appears for the first time in the Zimnegorsk Formation. However, insufficiently reliable stratigraphic and facies affiliations of the Sylvitsa Group and the absence of isotopic datings remained serious obstacles for such correlation until recently.

In 2002, we found thin volcanic ash beds in the upper part of the Staropechny Formation. These beds are associated with the chocolate brown thin-bedded mudstones that crop out on the left bank of the Sylvitsa River downstream of the Kernos Creek. In 2003, volcanic ash beds, which are also closely related to the chocolate brown mudstones, were revealed in the Staropechny and Perevalok formations and in the lower subformation of the Chernokamen Formation in the Vilukha ravine on the left and right banks of the Us'va River. In 2004, ash beds were traced for 4.5 km in the lower subformation of the Chernokamen Formation along the Mezhevaya Utka River. In all the above cases, ash beds were readily discernible as a poorly cemented light gray (with pinkish, cream, and greenish hues) rock among the host chocolate brown mudstones.

Members of chocolate brown mudstones with volcanic ash beds are important for Upper Vendian stratigraphy of the East European Platform. The tuffaceous rocks serve as key units for subdivision and correlation of outcrops and borehole sections [2, 3, 5, 6]. The most complete Upper Vendian platformal sections of the Mezen syneclise and the southeastern White Sea region

[a] *Zavaritsky Institute of Geology and Geochemistry, Uralian Division, Russian Academy of Sciences, Pochtovyi per. 7, Yekaterinburg, 620151 Russia; e-mail: ronkin@r66.ru*

[b] *Paleontological Institute, Russian Academy of Sciences, Profsoyuznaya ul. 123, Moscow, 117997 Russia*

[c] *Karpinsky All-Russia Research Institute of Geology, Srednii pr. 74, St. Petersburg, 199106 Russia*

include three key tuffaceous units (at the bases of the Lamitsa, Verkhovka, and Zimnegorsk formations). In the Sylvitsa Group of the Central Urals, chocolate brown mudstones with volcanic ash beds also occur at three stratigraphic levels: in the upper part of the Staropechny Formation, in the middle part of the Perevalok Formation, and in the lower subformation of the Chernokamen Formation. The occurrence of volcanic ash beds in the Sylvitsa Group, as well as data on the distribution of fossils and structure of the sedimentary sequence, allowed us to refine considerably the correlation of Upper Vendian sections on the western slope of the Central Urals with remote sections of the White Sea region. In this connection, the U–Pb zircon age of the youngest tuffaceous unit in the Chernokamen Formation is of special interest. This age has been determined by the SHRIMP II U–Pb dating method at the Center for Isotopic Studies of the All-Russia Geological Institute (St. Petersburg).

Microscopic examination of thin sections showed that volcanic tuffs are strongly altered basic or intermediate rocks with relict psammitic or pelitic-psammitic textures. They are mainly composed of angular or subangular clasts of volcanic rocks and glass (from 0.02–0.05 to 0.1–0.2 mm in size) and plagioclase fragments. With respect to texture and composition, they are subdivided into fine-grained lithoclastic (vitrocrystallo- or crystallovitrolithoclastic) and very fine-grained (crystallo- or lithocrystallovitroclastic) tuffs. Fragments of volcanic rocks are distinguished by a fine microlitic texture, which mostly can be defined as a hyaline texture. Intersertal texture and numerous small pores are also observed in some places. The angular or rounded glass fragments often contain fine pores filled with clay (less frequently, chlorite or prehnite aggregates). Open pores with acute edges are seen along the periphery of some volcanic glass fragments. As a rule, the reddish brown glass is poorly crystallized. The rounded grains of chlorite aggregates and sporadic quartz grains are seen together with the aforementioned clasts. All components mentioned above are replaced with clay minerals to a variable extent. The light gray or almost white color of groundmass in reflected light indicates the presence of montmorillonite. Some ash beds reveal a graded sorting of clastic material. The host chocolate brown mudstone consists of very fine clayey material, which is almost opaque owing to fine dissemination of hematite. Angular quartz fragments (<0.04 mm in size) and numerous fine muscovite flakes are discernible. The occurrence of beds mainly composed of basaltic, basaltic andesitic, and glassy fragments (80–90%) in the chocolate brown thin-bedded mudstone, acute edges of many glass fragments, and open pores therein indicate that the beds are pyroclastic materials deposited without any mechanical reworking in water. The XRD study of the fine (<0.001 mm) fraction of tuffaceous beds showed that no less than 20% of the rock volume is occupied by mixed-layer minerals of the smectite–illite type. No swelling phases were identified in host mudstones.

The ash bed of the Chernokamen Formation (Si/Al = 2.2–2.6) is comparable with high-alumina tuff of the Upper Vendian Redkino Horizon at the East European Platform [7]. Relative to the host mudstone, ash bed from the Chernokamen Formation is characterized by a much lower La_N/Yb_N ratio (3.73–6.68), depletion in HREE ($2.13 < Gd_N/Yb_N < 3.07$), a lower slope of the left branch of the plot ($1.64 < La_N/Sm_N < 2.56$), and a relatively small negative Eu anomaly (Eu/Eu* > 0.80).

Zircons were separated from ash bed samples after their crushing, sieving, and shaking, isodynamic magnetic separator, and heavy liquids. The zircon grains for analysis were finally handpicked under a binocular microscope. The in situ U–Pb zircon dating was performed according to analytical procedures described in [8]. After fixing the chosen crystals together with SL13, 91500, and TEMORA standards by Epofix resin in a pellet (~25 mm in diameter), the latter was polished until the exposure of the crystals. Then, a scanning electron method was used to obtain cathodoluminescence images of the zircon structure (Fig. 1) and to select coordinates of the points suitable for local microprobe analysis. Points for analysis were chosen by means of visual navigation based on the intensity of light and dark (enriched in uranium) zones. After completion of adjustment and calibration, the Pb isotopic composition and U/Pb ratio were measured in standard zircon. The obtained results were used further as reference values for calculation of the U–Pb age of a sample. Five to seven spectra of $^{90}Zr_2{}^{16}O$, ^{204}Pb, ^{206}Pb, ^{207}Pb, ^{208}Pb, ^{238}U, $^{232}Th^{16}O$, and $^{238}U^{16}O$ mass peaks were recorded at each analysis point. The Pb isotopic composition and U/Pb ratio in a chosen point were measured for 10–15 min to reach the necessary level of statistical uncertainty. Measurements of TEMORA, 91500, and SL13 zircon standards were repeated after 4–5 analyses of the zircons. The results obtained were processed with SQUID and ISOPLOT/EX software packages. The results of in situ U–Pb zircon dating are presented in the table and Fig. 2.

Zircons separated from ash beds turned out to be heterogeneous and can be separated into two groups. The first group comprises euhedral and subhedral crystals with a coefficient of elongation equal to 2.8, while the second group includes isometric grains with or without inclusions. These groups include both homogeneous and heterogeneous grains with respect to cathodoluminescence. Some crystals demonstrate a distinct zoning. The U content is relatively low (43–359 ppm).

The $^{207}Pb/^{235}U$–$^{206}Pb/^{238}U$ plot (Fig. 2) shows that SHRIMP II data points define a discordia passing through six craters of zircons (Us272.1.1, Us272.5.1, Us272.2.1, Us272.3.1, Us272.7.1, and Us272.8.1). The upper intercept of this discordia with concordia yields an age of 557 ± 13 Ma (2σ, MSWD = 0.18, probability 0.95), while the lower intercept corresponds to the zero

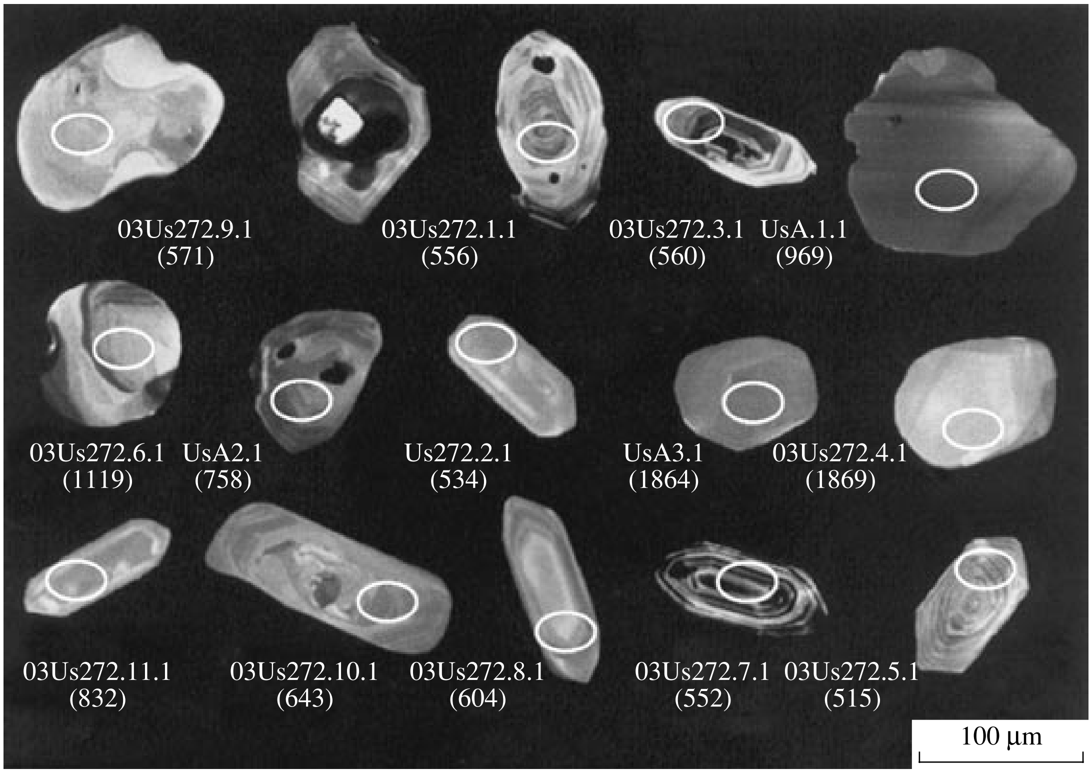

Fig. 1. Cathodoluminescence images of zircons extracted from ash interbed at the base of the Chernokamen Formation (sample Us272) and host mudstone (sample UsA). The section along the right bank of the Us'va River upstream from the Vilukha Ravine. The white elliptic contour demonstrates the location of the crater within the crystal. Numerals in parentheses indicate the $^{207}Pb/^{206}Pb$ age, Ma.

value within uncertainty limits. The overlapping ellipses, which correspond to the U–Pb SHRIMP II data for craters Us272.7.1 and Us272.8.1, yield concordant age of 557 ± 10 Ma (2σ, MSWD = 0.0042, probability 0.95). Other data points (Us272.10.1, Us272.9.1, Us272.11.1, Us272.6.1, and Us272.4.1) make up three age clusters with much older $^{207}Pb/^{206}Pb$ values (up to 1868 ± 24 Ma). To clarify the nature of the older U–Pb data, we determined the age of zircons separated from the host chocolate brown mudstones (sample UsA). The results obtained are in good agreement with three pre-Vendian age clusters of zircon crystals from ash beds.

The obtained SHRIMP II results suggest that the U–Pb systematics on zircons Us272.1.1, Us272.5.1, Us272.2.1, Us272.3.1, Us272.7.1, and Us272.8.1 yield regression line of 557 ± 13 Ma (2σ, MSWD = 0.18), which is consistent with geological data. This age of zircons from the base of the Chernokamen Formation may be correlated with the age of granitoids from the basement of the Pechora Terrain (557 ± 6 Ma) that was emplaced at the final stage of the Timanian orogeny at the northeastern margin of the Baltica paleocontinent [9]. The remaining analyzed zircon crystals are inherited formations, and they define the age of rocks in provenance(s). The age clusters include both pre-Riphean and younger materials. The pre-Riphean material is related to the release of zircons (or their mobilization during eruption) from the basement rocks of the East European Platform and their introduction to sediments. The younger material indicates the presence of Middle and Late Riphean rocks in the drainage areas. Since Late Riphean–Early Vendian igneous complexes are widespread in the Kvarkush–Kamennogorsk anticlinorium [10], it may be suggested that zircons estimated at ~680 Ma were also derived from local provenances.

Analysis of structure and depositional setting of rocks of the Sylvitsa Group shows that the lower subformation of the Chernokamen Formation, which contains ash bed of the third tuffaceous unit, is a large depositional system. This system is bounded from below and above by stratigraphic unconformities that are reflected in abrupt changes of the facies structure of sedimentary rocks and the character of sedimentary basin. The lower boundary marks transition from an open basin with relatively quiet hydrodynamic regime (Perevalok Formation) to the high-energy fluviomarine sediments of a relatively isolated basin. The distinctly transgressive pattern of the upper boundary is emphasized by prodeltaic sediments of the middle subformation. These sediments overlap different stratigraphic units of the lower subformation of the Chernokamen Formation and abruptly give way to a thick sequence

In situ U–Pb (SHRIMP II) data on zircons in ash beds and host mudstones (Upper Vendian Chernokamen Formation, Sylvitsa Group, Central Urals)

Sample crystal crater	$^{206}Pb_c$, %	U	Th	$^{232}Th/^{238}U$	$^{206}Pb^*$, ppm	(1) $^{238}U/^{206}Pb^*$ (±%)	(1) $^{207}Pb^*/^{206}Pb^*$ (±%)
		ppm					
Us272.1.1	–	154	135	0.91	4.91	26.70 (1.5)	0.0587 (7.4)
Us272.5.1	0.47	128	105	0.85	5.14	21.54 (1.5)	0.0576 (8.3)
Us272.2.1	0.23	94	65	0.71	4.64	17.48 (1.6)	0.0581 (7.6)
Us272.3.1	–	154	153	1.03	9.41	14.06 (1.2)	0.0588 (3.0)
Us272.7.1	0.37	240	102	0.44	18.3	11.31 (2.8)	0.0586 (3.4)
Us272.8.1	3.26	114	52	0.48	9.31	10.83 (2.8)	0.0600 (6.5)
Us272.10.1	–	169	291	1.78	16.0	9.10 (1.1)	0.0611 (2.0)
Us272.9.1	1.82	53	71	1.38	5.44	8.55 (2.0)	0.0591 (9.0)
Us272.11.1	0.01	56	69	1.26	5.45	8.89 (2.0)	0.0668 (9.8)
Us272.6.1	–	43	30	0.71	6.69	5.51 (1.9)	0.0769 (3.0)
Us272.4.1	0.12	91	40	0.46	26.9	2.892 (1.2)	0.1143 (1.3)
UsA.2.1	0.26	131	50	0.39	14.4	7.85 (2.6)	0.0645 (3.6)
UsA.1.1	0.10	359	108	0.31	53.4	5.792 (1.1)	0.0714 (1.7)
UsA.3.1	0.11	129	64	0.51	37.5	2.967 (2.3)	0.1140 (2.5)

Sample crystal crater	(1) $^{207}Pb^*/^{235}U$ (±%)	(1) $^{206}Pb^*/^{238}U$ (±%)	(1) $^{206}Pb/^{238}U$	(1) $^{207}Pb/^{206}Pb$	(1) $^{208}Pb/^{232}Th$	*Rho*	*D*, %
			Ma				
Us272.1.1	0.303 (7.6)	0.03745 (1.5)	237 ± 3.6	556 ± 161	253 ± 11	0.20	135
Us272.5.1	0.369 (8.5)	0.04642 (1.5)	293 ± 4.5	515 ± 182	311 ± 15	0.18	76
Us272.2.1	0.458 (7.8)	0.05721 (1.6)	359 ± 5.9	534 ± 166	394 ± 20	0.21	49
Us272.3.1	0.576 (3.0)	0.07115 (1.2)	443 ± 5.5	560 ± 65	462 ± 10	0.40	26
Us272.7.1	0.714 (3.4)	0.0884 (2.8)	546 ± 16	552 ± 74	517 ± 19	0.82	1
Us272.8.1	0.763 (6.6)	0.0923 (2.8)	569 ± 17	604 ± 141	526 ± 43	0.43	6
Us272.10.1	0.925 (2.3)	0.1099 (1.1)	672 ± 7.8	643 ± 43	673 ± 11	0.55	–4
Us272.9.1	0.953 (9.2)	0.1170 (2.0)	713 ± 15	571 ± 196	710 ± 29	0.22	–20
Us272.11.1	1.040 (10)	0.1125 (2.0)	687 ± 14	832 ± 204	711 ± 37	0.20	21
Us272.6.1	1.924 (3.5)	0.1815 (1.9)	1075 ± 22	1119 ± 60	1145 ± 36	0.63	4
Us272.4.1	5.447 (1.8)	0.3457 (1.2)	1914 ± 27	1869 ± 23	1912 ± 45	0.92	–2
UsA.2.1	1.132 (3.6)	0.1273 (2.6)	772 ± 21	758 ± 76	772 ± 29	0.72	–2
UsA.1.1	1.699 (1.7)	0.1727 (1.1)	1027 ± 12	969 ± 35	1037 ± 22	0.65	–6
UsA.3.1	5.300 (2.5)	0.3371 (2.3)	1873 ± 50	1864 ± 46	1847 ± 49	0.92	–0.5

Note: Uncertainities ±2σ; (Pb_c, Pb*) common and radiogenic lead, respectively. Calibration uncertainties relative to standards are 0.4%. (1) Correction based on ^{204}Pb; (*D*) discordance; (*Rho*) correlation coefficient.

deposited in the relatively shallow-water distal setting of a flat, open deltaic plain.

The lower subformation of the Chernokamen Formation includes the youngest tuffaceous unit in the Vendian section of the Central Urals (U–Pb zircon age 557 ± 13 Ma). This fact, together with the taxonomic composition of fossil biota, suggest the following most probable correlation of the studied stratigraphic subdivision with Upper Vendian reference sections of the southeastern White Sea region. The lower subformation of the Chernokamen Formation may be correlated with the Zimnegorsk Formation (White Sea region), which also contains the third tuffaceous unit at its base [6, 11]. Our U–Pb zircon dating of the ash interbed at the base of the Chernokamen Formation is consistent with the U–Pb zircon age (555.3 ± 0.3 Ma) of volcanic ash from the Zimnegorsk Formation [11, 12]. Furthermore, the base of the middle subformation of the Cher-

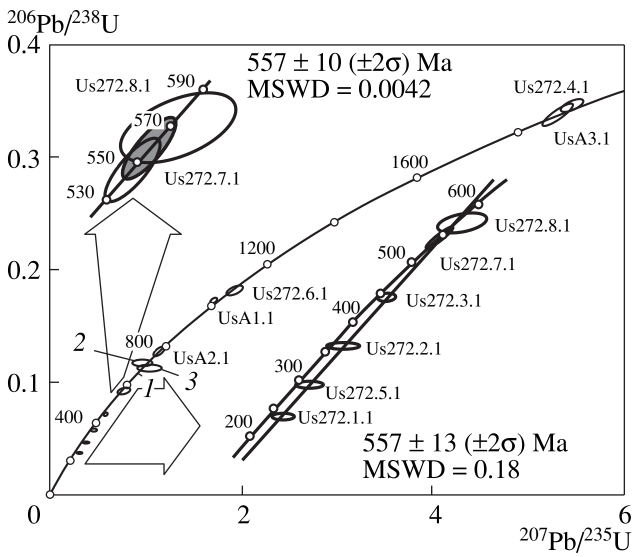

Fig. 2. U–Pb (SHRIMP II) data on zircons from ash interbed at the base of the Chernokamen Formation (sample Us272) and host mudstone (sample UsA). Ellipses *1, 2*, and *3* correspond to craters Us272.10.1, Us272.9.1, and Us272.11.1, respectively.

nokamen Formation contains the remains of soft-bodied organisms *Yorgia* [4], which are characteristic of the upper part of the Zimnegorsk Formation and the lower part of the Yorga Formation in the White Sea region [13].

Thus, the proposed correlation converges the levels and surfaces bounding the lower subformation of the Chernokamen Formation and the Zimnegorsk Formation. These are the sequence boundaries related to eustatic oscillations of the sea level. Their consideration may be crucial for interbasinal stratigraphic correlation and reconstruction of the Neoproterozoic time interval.

ACKNOWLEDGMENTS

This work was supported by the Russian Foundation for Basic Research (project nos. 03-05-64121 and 06-05-64223), the Natural Environment Research Council (grant NER/A/2001/01049), and the Program of the Division of Earth Sciences of the Russian Academy of Sciences “Isotopic Systems and Isotopic Fractionation in Natural Processes.” D. Grazhdankin acknowledges the Irish Research Council for Science, Engineering, and Technology (IRCSET) Postdoctoral Fellowship at University College, Dublin.

REFERENCES

1. B. D. Ablizin, M. L. Klyuzhina, F. A. Kurbatskaya, and A. M. Kurbatskii, *Upper Riphean and Vendian on the Western Slope of the Central Urals* (Nauka, Moscow, 1982) [in Russian].
2. V. V. Kirsanov, Izv. Akad. Nauk SSSR, Ser. Geol., No. 6, 86 (1968).
3. E. M. Aksenov, in *The Vendian System* (Nauka, Moscow, 1985), vol. 2: Stratigraphy and Geologic Processes, pp. 3–34 [in Russian].
4. D. V. Grazhdankin, A. V. Maslov, T. M. R. Mustill, and M. T. Krupenin, Dokl. Earth Sci. **401A**, 382 (2005) [Dokl. Akad. Nauk **401**, 784 (2005)].
5. E. M. Aksenov and S. A. Volkova, Dokl. Akad. Nauk SSSR **188**, 635 (1969).
6. A. F. Stankovskii, E. M. Verichev, and I. P. Dobeiko, in *The Vendian System* (Nauka, Moscow, 1985), vol. 2: Stratigraphy and Geologic Processes, pp. 67–76 [in Russian].
7. D. V. Borkhvardt and S. B. Felitsyn, Volkanol. Seismol., No. 1, 33 (1992).
8. Yu. L. Ronkin, D. I. Matukov, S. L. Presnyakov, et al., Litosfera, No. 1, 135 (2005).
9. V. Pease, E. Dovshikova, L. Beliakova, and D. G. Gee, Geol. Soc. London Mem. **30**, 75 (2004).
10. G. A. Petrov, A. V. Maslov, and Yu. L. Ronkin, Litosfera, No. 4, 42 (2005).
11. D. V. Grazhdankin, Stratigr. Geol Correlation **11** (4), 313 (2003) [Stratigraf. Geol. Korrelyatsiya **11** (4), 3 (2003)].
12. M. W. Martin, D. V. Grazhdankin, S. A. Bowring, et al., Science **288**, 841 (2000).
13. D. Grazhdankin, Paleobiology **30**, 203 (2004).